Spherical Vector Wave Expansion of Gaussian Electromagnetic Fields for Antenna-Channel Interaction Analysis

Alayon Glazunov, Andres; Gustafsson, Mats; Molisch, Andreas; Tufvesson, Fredrik; Kristensson, Gerhard

2008

LUND UNIVERSITY

PO Box 117
221 00 Lund
+46 46-222 00 00

CODEN:LUTEDX/(TEAT-7162)/1-28/(2008)

Spherical Vector Wave Expansion of Gaussian Electromagnetic Fields for Antenna-Channel Interaction Analysis

Andrés Alayón Glazunov, Mats Gustafsson, Andreas F. Molisch, Fredrik Tufvesson, and Gerhard Kristensson

Electromagnetic Theory
Department of Electrical and Information Technology
Lund University
Sweden

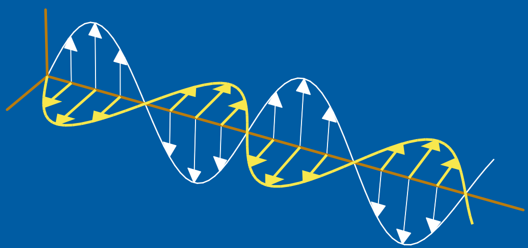

Andrés Alayón Glazunov
Andres.Alayon@eit.lth.se

Fredrik Tufvesson
Fredrik.Tufvesson@eit.lth.se

Department of Electrical and Information Technology
Radio Communications
P.O. Box 118
SE-221 00 Lund
Sweden

Mats Gustafsson
Mats.Gustafsson@eit.lth.se

Gerhard Kristensson
Gerhard.Kristensson@eit.lth.se

Department of Electrical and Information Technology
Electromagnetic Theory
Lund University
P.O. Box 118
SE-221 00 Lund
Sweden

Andreas F. Molisch
Andreas.Molisch@eit.lth.se

Department of Electrical and Information Technology
Radio Communications
P.O. Box 118
SE-221 00 Lund
Sweden

and

Mitsubishi Electric Research Labs
Cambridge, MA 02139
USA

Editor: Gerhard Kristensson

Abstract

In this paper we introduce an approach to analyze the interaction between antennas and the propagation channel. We study both the antennas and the propagation channel by means of the spherical vector wave mode expansion of the electromagnetic field. Then we use the expansion coefficients to study some properties of general antennas in those fields by means of the antenna scattering matrix. The focus is on the spatio-polar characterization of antennas, channels and their interactions. We provide closed form expressions for the covariance of the field multi-modes as function of the Power Angle Spectrum (PAS) and the channel cross-polarization ratio (XPR). A new interpretation of the Mean Effective Gains (MEG) of antennas is also provided. The maximum MEG is obtained by conjugate mode matching between the antennas and the channel; we also prove the (intuitive) results that the optimum decorrelation of the antenna signals is obtained by the excitation of orthogonal spherical vector modes.

1 Introduction

Space has been declared by many as the “final frontier" in wireless communications, while others recognize its exploitation as just “important and fruitful". In any case, its importance is without a doubt indisputable. Then, a natural question is: How can we “squeeze" the last bit of information from the “Space"? In order to answer this question and many others, we need to understand the fundamental issues of the problem posed. In particular the physical properties of both antennas and propagation channels. More precisely, here, we are interested in the interplay between antennas and the radio propagation channel. Our final goal is to understand the actual physical implications of the spatial and polarization selectivity of the propagation channel on the communication link capacity.

In most practical situations the radio propagation channel is selective in both space and polarization[1], i.e., within some volume it is more likely to receive signals from some directions rather than others as well as with some polarization rather than others. This has, as we are going to see, a great impact on the modes excited in the channel and therefore also on the antennas we should use in those channels. Hence, it is important to study the properties of the field incident at the antenna in order to understand the interaction between the antenna field the field of the waves impinging at it.

There have been other papers aiming to describe the interaction between the antennas and the channel in terms of multimode expansions [25], [26], [24], [23], [20], [19], [13], [14]. However, these approaches are restricted to the scalar case, where the polarization characteristics of the channel are omitted. This of course, does not suffice for the full understanding of the physics involved in the interaction between the wireless communication channel and the antennas. The limitations of such an

[1]Selectivity in time is of course also of great relevance, but we are not going to deal with it here, see [3] for further reference on channel properties.

approach are detrimental to both the theoretical treatment of electromagnetic fields, since they are inherently vector fields, and the practical applications, since polarization diversity is gaining more and more importance for wireless communications and requires proper modelling [21].

A natural way to express the polarization, angle, and spatial diversity inherent to MIMO systems [28], [10], is by describing the properties of both antennas and channels by means of the spherical vector wave expansion of the electromagnetic field, which is a particular solution to Maxwell equations [17], [15]. This expansion gives a condensed interpretation of the radiation properties of an antenna. Although this mode expansion is infinite, in practice, it is sufficient to consider a finite set of modes due to the high Q-factors (strong reactive near field), and hence high losses and low bandwidth, associated with high order modes [5]. Moreover, the spherical vector waves expansion and the scattering matrix representation of an antenna are the cornerstone of the theory and practice of near-field antenna measurements [15]. This approach has also recently been successfully applied to the problem of the interaction of antennas with the radio channel, where as a first assumption an isotropic unpolarized field[2] was assumed for the incoming field [11]. It was shown there that for the isotropic field[3] the excited spherical modes are all of equal magnitude.

In this paper we model the field incident at the antenna by a mixed Gaussian vector field consisting of an unpolarized stochastic component with non-isotropic power angular spectra (PAS) and a deterministic (polarized) component. The power imbalance of orthogonal polarizations is modelled by the channel cross-polarization ratio (XPR). The Gaussianity of the field is defined with respect to the complex vector field amplitudes of the incident field. We develop a model for the correlation between the field components under these assumptions. We then use this model to derive the statistical properties of the expansion coefficients in spherical vector modes for general Gaussian fields and the properties of optimal antennas in those fields.

Our paper aims at developing some insights into the physics involved in the wireless communication, and, in the process, provide criteria and methods for optimally matching antennas to a given channel. The key contributions of our paper on the latter aspect can be summarized as follows:

- we show that maximum Mean Effective Gain (MEG) and the maximum received (transmitted) power of an antenna is achieved by conjugate mode matching
- we show that independent signals are achieved by eigenmode reception (transmission) over the strongest multimodes.

Other relevant contributions are the following:

[2]The coherence matrix $\mathbf{J}$ of the field with orthogonal field components E_α and E_β has elements $J_{\alpha\beta} = \langle E_\alpha E_\beta^* \rangle$. We say then that the field is polarized when $\det(\mathbf{J}) = \mathbf{0}$ and that the field is unpolarized when $J_{\alpha\beta} = J_{\beta\alpha} = 0$.

[3]In this paper, an isotropic field is understood as a field where the AoAs (angle of arrivals) are uniformly distributed over the sphere of unit radius.

- we show that in a Gaussian electromagnetic field (the propagation channel) each multimode coefficient in the spherical vector wave expansion is a Gaussian variate and as a consequence we prove that the envelope of each multimode coefficient in the spherical vector wave expansion is a Ricean variate.

- we derive closed-form expressions for the mode correlation matrix for arbitrary PAS of incoming waves and for the normalized power of single modes in terms of the PAS of incoming waves and the channel XPR.

The remainder of the paper is organized as follows. In Section 2, we give a brief description of the statistical properties of the model used for the incident field. In Section 3, we express the same in terms of the expansion coefficients, where we also provide closed form expressions for the elements of the spherical vector wave mode correlation matrix. Section 4 describes the scattering matrix representation of the joint antenna-channel properties, and we also derive some fundamental properties of antennas such as Mean Effective Gain. In Section 5, we provide simulation results where we study the interaction between a Gaussian channel with Laplacian PAS and patch and tripole antennas. The conclusions are summarized in Section 6.

2 Incident Field

The wireless communication channel is often modelled as the superposition of random waves. Under certain conditions the envelope of the resulting signal is distributed according to the Rayleigh probability density function (pdf) while the phases are uniformly distributed. This results in an unpolarized total field. More specifically, Rayleigh fading may be seen as an ensemble of Gaussian random waves, made up from superpositions of plane waves with random phases at each position in space. The directions of arrivals (DoAs) are in general non-isotropically distributed on the sphere of unit radius. Thus, the electric field $\boldsymbol{E}$ at position $\boldsymbol{r}$, can be expressed through the plane wave spectrum (PWS) representation

$$\boldsymbol{E}(\boldsymbol{r}) = \int \tilde{\boldsymbol{E}}_0(\hat{\boldsymbol{k}}) \mathrm{e}^{-\mathrm{i}k\hat{\boldsymbol{k}}\cdot\boldsymbol{r}} \mathrm{d}\Omega, \tag{2.1}$$

where the integral is taken over the sphere of unit radius, $\mathrm{d}\Omega$ is the elementary solid angle, $\tilde{\boldsymbol{E}}_0(\hat{\boldsymbol{k}})$ denotes the random complex PWS of the field $\boldsymbol{E}(\boldsymbol{r})$ at the observation point in space $\boldsymbol{r}$, $k = 2\pi/\lambda$ is the wave number, $\hat{\boldsymbol{k}}$ is the unit wave vector in the direction of the plane wave propagation, λ is the wave length, and the time convention $\mathrm{e}^{\mathrm{i}\omega t}$ is assumed.

The more general Ricean fading model assumes a deterministic, and therefore polarized, component in addition to the random component. In general, its amplitude is larger than the amplitude of each the single unpolarized waves. In this case, the PWS of the total field is given by the vector

$$\tilde{\boldsymbol{E}}_0(\hat{\boldsymbol{k}}) = \tilde{\boldsymbol{E}}_{\mathrm{pol}}(\hat{\boldsymbol{k}}) + \tilde{\boldsymbol{E}}_{\mathrm{unpol}}(\hat{\boldsymbol{k}}), \tag{2.2}$$

where $\tilde{\boldsymbol{E}}_{\rm pol}(\hat{\boldsymbol{k}})$ is the deterministic component while $\tilde{\boldsymbol{E}}_{\rm unpol}(\hat{\boldsymbol{k}})$ is the zero mean random field component with $\langle\tilde{\boldsymbol{E}}_{\rm unpol}(\hat{\boldsymbol{k}})\rangle = 0$ and $\langle.\rangle$ denotes the ensemble average see, e.g., [22], p.285). We model $\tilde{\boldsymbol{E}}_0(\hat{\boldsymbol{k}})$ as a stochastic process that assigns to every observation ς of $\tilde{\boldsymbol{E}}_0$ the family of functions $\tilde{\boldsymbol{E}}_0(\hat{\boldsymbol{k}},\varsigma)$. Hence, ς is the actual realization (observation) of the random variable $\tilde{\boldsymbol{E}}_0$. Then, representing $\tilde{\boldsymbol{E}}_0$ through orthogonal PWS field components $\tilde{E}_{0\alpha}(\hat{\boldsymbol{k}})$ and $\tilde{E}_{0\beta}(\hat{\boldsymbol{k}})$, the average of the polarization components are

$$\langle\tilde{E}_{0\alpha}(\hat{\boldsymbol{k}})\rangle = E_{{\rm pol}\alpha}(\hat{\boldsymbol{k}}_0)\delta^2(\hat{\boldsymbol{k}}-\hat{\boldsymbol{k}}_0), \tag{2.3}$$

for the $\tilde{E}_{0\alpha}(\hat{\boldsymbol{k}})$ component, where $E_{{\rm pol}\alpha}(\hat{\boldsymbol{k}}_0)$ is one of the two orthogonal components of the polarized field component that arrives from direction $\hat{\boldsymbol{k}}_0$; a similar expression applies to the $\tilde{E}_{0\beta}(\hat{\boldsymbol{k}})$ component. The symbol $\delta^2(\hat{\boldsymbol{k}}) = \delta(\theta)\delta(\phi)/\sin(\theta)$ denotes the Dirac-delta in spherical coordinates defined on the sphere of unit radius.

We postulate the following correlation model for the PWS, which is an extension of the model in [4], [18], [9]:

1. The phases of the co-polarized PWS components are uncorrelated for different DoAs, $\hat{\boldsymbol{k}}$ and $\hat{\boldsymbol{k}}'$. This is the random PWS field for which the two orthogonal components, $\tilde{E}_{{\rm unpol}\alpha}(\hat{\boldsymbol{k}})$ and $\tilde{E}_{{\rm unpol}\alpha}(\hat{\boldsymbol{k}}')$ or $\tilde{E}_{{\rm unpol}\beta}(\hat{\boldsymbol{k}})$ and $\tilde{E}_{{\rm unpol}\beta}(\hat{\boldsymbol{k}}')$ are uncorrelated.

2. The phases of the cross-polarized PWS are uncorrelated for different DoAs, $\hat{\boldsymbol{k}}$ and $\hat{\boldsymbol{k}}'$, with the exception of one fixed direction $\hat{\boldsymbol{k}}_0$. This is the deterministic PWS field component, for which the two orthogonal components $\tilde{E}_{{\rm pol}\alpha}(\hat{\boldsymbol{k}})$ and $\tilde{E}_{{\rm pol}\beta}(\hat{\boldsymbol{k}}')$ or $\tilde{E}_{{\rm pol}\beta}(\hat{\boldsymbol{k}})$ and $\tilde{E}_{{\rm pol}\alpha}(\hat{\boldsymbol{k}}')$ are correlated.

Therefore, if $\tilde{\boldsymbol{E}}_{0\alpha}(\hat{\boldsymbol{k}})$ and $\tilde{\boldsymbol{E}}_{0\beta}(\hat{\boldsymbol{k}})$, are the complex PWS components of the random electric field in two orthogonal polarizations, then

$$\begin{aligned}\langle\tilde{E}_\alpha(\hat{\boldsymbol{k}})\tilde{E}^*_\beta(\hat{\boldsymbol{k}}')\rangle &= E_{{\rm pol},\alpha}(\hat{\boldsymbol{k}}_0)E^*_{{\rm pol},\beta}(\hat{\boldsymbol{k}}_0)\delta^2(\hat{\boldsymbol{k}}-\hat{\boldsymbol{k}}_0)\delta^2(\hat{\boldsymbol{k}}'-\hat{\boldsymbol{k}}_0)\\ &\quad+\langle|E_{{\rm unpol},\alpha}(\hat{\boldsymbol{k}}')|^2\rangle\delta^2(\hat{\boldsymbol{k}}-\hat{\boldsymbol{k}}')\delta_{\alpha\beta},\end{aligned} \tag{2.4}$$

where $\delta_{\alpha\beta}$, denotes the Kronecker-delta function and the asterisk $(.)^*$denotes complex conjugate.

The above stated conditions define both the auto- and cross-correlation properties of the random PWS field $\boldsymbol{E}_0$, i.e., the second order properties of the modelled stochastic field, at different DoAs $\hat{\boldsymbol{k}}$ and $\hat{\boldsymbol{k}}'$. It is worthwhile to note that the physical meaning of the cross-correlation of the incoming field evaluated at different DoAs defined in (2.4), relies on the assumption that the vector field components themselves are described by Gaussian stochastic processes in the direction of arrivals. It should be observed that (2.4) is independent from the choice of coordinate system. However, in practice, it is often convenient to define the directional properties of both the antenna and the propagation channel in some specific coordinate system.

Hence, the PAS of the unpolarized field component along $\hat{\boldsymbol{\theta}}$ or $\hat{\boldsymbol{\phi}}$, which are the two orthogonal orientations in the spherical coordinate system are defined according to the definition given in [18]. The PAS depends upon the directions of arrival Ω, where Ω is used interchangeably to denote the set of spherical coordinates (θ, ϕ) and the solid angle and describe the DoA defined by the vector $\hat{\boldsymbol{k}}$ expressed in the same system. Commonly, the PASs of field components along $\hat{\boldsymbol{\theta}}$ and $\hat{\boldsymbol{\phi}}$ are denoted $P_\theta(\Omega)$ and $P_\phi(\Omega)$, respectively. Then, the PAS of the unpolarized field component is given by

$$\langle |E_{\mathrm{unpol},\theta}(\Omega)|^2 \rangle = \frac{\eta k^2}{2\pi} P_{\mathrm{unpol},\theta} p_\theta(\Omega), \tag{2.5}$$

where k is the wave number of the incoming plane wave, η is the free-space impedance[4], $P_{\mathrm{unpol},\theta}$ is the power that would be received by an isotropic antenna polarized along $\hat{\boldsymbol{\theta}}$ a similar expression applies for the component along $\hat{\boldsymbol{\phi}}$, $\langle |E_{\mathrm{unpol},\phi}(\Omega)|^2 \rangle$. The pdfs $p_\theta(\Omega)$ and $p_\phi(\Omega)$ satisfy the normalization $\int p_\alpha(\Omega) \mathrm{d}\Omega = 1$, where α stands for either θ or ϕ.

Similarly, the PAS of the polarized field component along $\hat{\boldsymbol{\theta}}$ and $\hat{\boldsymbol{\phi}}$ in spherical coordinates is

$$\langle |E_{\mathrm{pol},\theta}(\Omega)|^2 \rangle = \frac{\eta k^2}{2\pi} P_{\mathrm{pol},\theta} \delta^2(\Omega - \Omega_0), \tag{2.6}$$

where $P_{\mathrm{pol},\theta}$ is the average power that would be received by an isotropic antenna polarized along $\hat{\boldsymbol{\theta}}$ at the incidence direction, Ω_0, of the polarized, deterministic component where $\delta^2(\Omega) = \delta(\theta)\delta(\phi)/\sin(\theta)$ is the Dirac-delta; a similar expression applies for the component along $\hat{\boldsymbol{\phi}}$, $\langle |E_{\mathrm{pol},\phi}(\Omega)|^2 \rangle$.

Ricean channels are characterized by the Ricean K-factor, which is defined as the ratio of the power in the deterministic component to the power of the stochastic component of the received signals. Here, we follow the same formalism and define the effective Ricean K-factor as the ratio of the power in the polarized component to the power in the unpolarized component

$$K = \frac{P_{\mathrm{pol}}}{P_{\mathrm{unpol}}} = \frac{\chi_{\mathrm{unpol}} K_\theta + K_\phi}{\chi_{\mathrm{unpol}} + 1}, \tag{2.7}$$

where $P_{\mathrm{pol}} = P_{\mathrm{pol},\theta} + P_{\mathrm{pol},\phi}$, $P_{\mathrm{unpol}} = P_{\mathrm{unpol},\theta} + P_{\mathrm{unpol},\phi}$, $K_\theta = \frac{P_{\mathrm{pol},\theta}}{P_{\mathrm{unpol},\theta}}$ and $K_\phi = \frac{P_{\mathrm{pol},\phi}}{P_{\mathrm{unpol},\phi}}$ are the K-factors of field components in the direction of $\hat{\boldsymbol{\theta}}$ or $\hat{\boldsymbol{\phi}}$, respectively. $\chi_{\mathrm{unpol}} = \frac{P_{\mathrm{unpol},\theta}}{P_{\mathrm{unpol},\phi}}$ is the XPR of the unpolarized field component. The effective Ricean factor is a measure of the power in the polarized component relative to the power of the unpolarized component.

The "effective" cross-polarization ratio of the channel XPR of the total field is defined as the ratio between the power in the $\hat{\boldsymbol{\theta}}$ polarization to the power in the $\hat{\boldsymbol{\phi}}$ polarization

$$\chi = \frac{P_{\mathrm{pol},\theta} + P_{\mathrm{unpol},\theta}}{P_{\mathrm{pol},\phi} + P_{\mathrm{unpol},\phi}} = \chi_{\mathrm{unpol}} \frac{K_\theta + 1}{K_\phi + 1}. \tag{2.8}$$

The fundamental statistical properties of the Gaussian vector field can then be summarized by the following quantities:

[4] We also use η to denote radiation efficiency.

- PAS of the field at two orthogonal polarizations, $P_\theta(\Omega)$ and $P_\phi(\Omega)$
- XPR of the channel, χ
- Ricean K-factor

The PAS of the unpolarized field plays a key role in propagation modelling since it describes, together with the power of the polarized component, the polarization- and spatial selectivity of the channel. Models of the PAS are usually derived by extensive measurements and reflect an average behavior of the propagation channel. They are usually used in both link and system level simulations of communications systems exploiting smart antennas or in general MIMO antenna systems [21]. However, they also find their use in computations of the mean effective gain of antennas (MEG), which is a measure of the performance of antennas in different propagation environments [27]. Below it is shown to be a fundamental measure of the antenna-channel interaction.

3 Spherical vector wave expansion of the incident field

The field impinging on an antenna can be modelled by the spherical vector wave expansion formalism. Hence, the total incident field is expanded in regular spherical vector waves $\mathbf{v}_{\tau ml}(k\boldsymbol{r})$ [17], [15]

$$\boldsymbol{E} = k\sqrt{2\eta}\sum_{l=1}^{\infty}\sum_{m=-l}^{l}\sum_{\tau=1}^{2} f_{\tau ml}\mathbf{v}_{\tau ml}(k\boldsymbol{r}), \tag{3.1}$$

for $|\boldsymbol{r}| \geq a$, where a is the radius of a sphere circumscribing the antenna and $f_{\tau ml}$ are the expansion coefficients corresponding to multi-poles or modes described by indices (τ, m, l). Whenever necessary, the multi–index ι is identified with the ordered number $\iota = 2(l^2 + l - 1 + m) + \tau$. Hence, the expansion coefficients f_ι can be represented by the vector $\boldsymbol{f}$. The multi–poles are classified as either TE ($\tau = 1$) or TM ($\tau = 2$). The azimuthal and radial dependencies are given by the m and l index, respectively. The factor $k\sqrt{2\eta}$ is used to power normalize the expansion coefficients. The regular spherical vector waves $\mathbf{v}_{\tau ml}(k\boldsymbol{r})$ are briefly described in Appendix A.

The plane wave expansion coefficients in regular spherical vector waves can then be expressed as the sum of the polarized and unpolarized components

$$f_\iota = f_\iota^{\mathrm{pol}} + f_\iota^{\mathrm{unpol}}, \tag{3.2}$$

where the expansion coefficients for the polarized field component are given by

$$f_\iota^{\mathrm{pol}} = \frac{4\pi(-\mathrm{i})^{l-\tau+1}}{k\sqrt{2\eta}}\boldsymbol{E}_{\mathrm{pol}}(\hat{\boldsymbol{k}}_0)\cdot\boldsymbol{A}_\iota^*(\hat{\boldsymbol{k}}_0), \tag{3.3}$$

where we have used (2.3). For the unpolarized field component expansion coefficients are

$$f_\iota^{\text{unpol}} = \frac{4\pi(-\mathrm{i})^{l-\tau+1}}{k\sqrt{2\eta}} \int \tilde{\boldsymbol{E}}_{\text{unpol}}(\hat{\boldsymbol{k}}) \cdot \boldsymbol{A}_\iota^*(\hat{\boldsymbol{k}}) \mathrm{d}\Omega, \tag{3.4}$$

where the functions $\boldsymbol{A}_\iota(\hat{\boldsymbol{r}})$ are the spherical vector harmonics, see Appendix A.

Clearly the expansion coefficients are obtained as a linear combination of individual plane waves.

3.1 Statistical properties of mode expansion coefficients

Now, since the incident field is assumed to be a random field, we are interested in characterizing the statistics of the multimode expansion coefficients, f_ι, which are summarized in the following propositions.

Proposition 1. *In a multipath propagation environment characterized by a mixed field with both a random Gaussian, unpolarized, field component and one deterministic, polarized, field component, the correlation matrix of expansion coefficients of the total received field in regular spherical vector waves is given by the sum of the mode correlation matrices corresponding to the polarized and the unpolarized components, respectively*

$$\boldsymbol{\mathcal{R}}_f = \boldsymbol{f}_{\text{pol}} \boldsymbol{f}_{\text{pol}}^H + \langle \boldsymbol{f}_{\text{unpol}} \boldsymbol{f}_{\text{unpol}}^H \rangle \tag{3.5}$$

where $\boldsymbol{f}_{\text{pol}}$ and $\boldsymbol{f}_{\text{unpol}}$ are the vectors with elements f_ι^{pol} and f_ι^{unpol}, respectively. The elements of the correlation matrices are given by,

$$\mathcal{R}_{\iota\iota'} = \mathcal{R}_{\iota\iota'}^{\text{pol}} + \mathcal{R}_{\iota\iota'}^{\text{unpol}}, \tag{3.6}$$

where $\mathcal{R}_{\iota\iota'}^{\text{pol}}$ denotes the mode cross-correlation of the polarized deterministic component given by

$$\begin{aligned} \mathcal{R}_{\iota\iota'}^{\text{pol}} \;=\; & 4\pi(-\mathrm{i})^{l-l'-\tau+\tau'} \ldots \\ & \ldots (P_{0\theta} A_{\iota,\theta}^*(\Omega_0) A_{\iota',\theta}(\Omega_0) \\ & +2\,\mathrm{Re}\left\{ \sqrt{P_{0\theta} P_{0\phi}} A_{\iota,\theta}^*(\Omega_0) A_{\iota',\phi}(\Omega_0) \mathrm{e}^{\mathrm{i}\psi} \right\} \\ & +P_{0\phi} A_{\iota,\phi}^*(\Omega_0) A_{\iota',\phi}(\Omega_0)), \end{aligned} \tag{3.7}$$

where Re *denotes real part. In* (3.7) *we have used that $\left|E_\theta E_\phi^*\right| = \frac{\eta k^2}{2\pi}\sqrt{P_{0\theta}P_{0\phi}}$ and that ψ is a phase angle that depends on the polarization, e.g., $\psi = 0$, for a linearly polarized wave and $\psi = \pm\frac{\pi}{2}$ for circularly polarized waves. $\mathcal{R}_{\iota\iota'}^{\text{unpol}}$ denotes the cross-mode correlation corresponding to the unpolarized component given by*

$$\begin{aligned} \mathcal{R}_{\iota\iota'}^{\text{unpol}} \;=\; & 4\pi(-\mathrm{i})^{l-l'-\tau+\tau'} \ldots \\ & \ldots \int P_\theta p_\theta(\Omega) A_{\iota,\theta}^*(\Omega) A_{\iota',\theta}(\Omega) \\ & +P_\phi p_\phi(\Omega) A_{\iota,\phi}^*(\Omega) A_{\iota',\phi}(\Omega) \mathrm{d}\Omega, \end{aligned} \tag{3.8}$$

where we have used the definition of the PAS of the incoming waves at two perpendicular polarizations (2.6). *The derivation is given in Appendix B.*□

Lemma 3.1. *In a multipath propagation environment characterized by a mixed field with both random Gaussian, unpolarized, field components and one deterministic, polarized, field component, the expansion coefficients of the total received field in regular spherical vector waves, f_ι, are Gaussian variates with mean*

$$\langle f_\iota \rangle = \frac{4\pi(-\mathrm{i})^{l-\tau+1}}{k\sqrt{2\eta}} \langle \boldsymbol{E}_0(\hat{\boldsymbol{k}}_0) \cdot \boldsymbol{A}_\iota^* \rangle = f_\iota^{\mathrm{pol}}, \tag{3.9}$$

and variance

$$\langle |f_\iota|^2 \rangle = \left| f_\iota^{\mathrm{pol}} \right|^2 + \langle \left| f_\iota^{\mathrm{unpol}} \right|^2 \rangle, \tag{3.10}$$

where the mode powers of the polarized component are given by

$$\begin{aligned} P_\iota^{\mathrm{pol}} &= \left| f_\iota^{\mathrm{pol}} \right|^2 \\ &= 4\pi(\sqrt{P_{0\theta}}\,|A_{\iota,\theta}(\Omega_0)| + \sqrt{P_{0\phi}}\,|A_{\iota\phi}(\Omega_0)|)^2, \end{aligned} \tag{3.11}$$

and the mode powers of the unpolarized component are given by

$$\begin{aligned} P_\iota^{\mathrm{unpol}} &= \langle \left| f_\iota^{\mathrm{unpol}} \right|^2 \rangle \\ &= 4\pi \int P_\theta p_\theta(\Omega)\,|A_{\iota,\theta}(\Omega)|^2 \\ &\quad + P_\phi p_\phi(\Omega)\,|A_{\iota\phi}(\Omega)|^2 \,\mathrm{d}\Omega. \end{aligned} \tag{3.12}$$

Hence, the second moments, i.e., the mode powers, are given by

$$P_\iota = P_\iota^{\mathrm{pol}} + P_\iota^{\mathrm{unpol}}. \tag{3.13}$$

as shown in Appendix C.□

Remark 1. *In a multipath propagation environment characterized by a mixed field with both random Gaussian, unpolarized, field components and one deterministic, polarized, field component, the envelope of the expansion coefficients of the total received field in regular spherical vector waves, $|f_\iota|$, are Ricean variates with K-factor*

$$K_\iota = \frac{P_\iota^{\mathrm{pol}}}{P_\iota^{\mathrm{unpol}}}. \tag{3.14}$$

This result follows directly from Lemma 1.□

It is now clear that the power of the mode with index ι corresponding to the polarized component depends upon both the AoA and the power of incoming waves from that direction at each polarization (3.11). Similarly, the power of the mode with index ι corresponding to the unpolarized component depends upon both the distribution of AoA and the average power at each polarization (3.12). The physical meaning is straightforward, the mode power is the power that would be received on average by an ideal antenna able to receive only the mode with index ι.

In the special case when only the unpolarized field component is present, it follows from (3.12) that the mode cross-correlation is given by $\mathcal{R}_{\iota\iota'} = \mathcal{R}_{\iota\iota'}^{\mathrm{unpol}}$. Hence, the mode power is $P_\iota^{\text{unpol}} = \mathcal{R}_{\iota\iota}^{\text{unpol}}$. Further, for the isotropic model we arrive at, $\mathcal{R}_{\iota\iota'} = 2\pi\delta_{mm'}\delta_{ll'}$, where we have used the orthogonality properties of the spherical harmonics and used the following normalization for the power densities, $P_\theta = P_\phi = \frac{1}{2}$.

For the analysis, in this paper, of the antenna-channel interaction, the working assumption is that the incident field is an finite sum of plane waves. It is, however, well known that a plane has infinite power, but, for all practical applications the total received power as well as the number of useful multimodes is finite. Indeed, all practical antennas can be defined by a finite set of spherical vector wave expansion coefficients [15], [16]. Moreover, for electrically small antennas according to the Chu-Fano theory, only the lower order expansion coefficients are of interest, since the influence of higher order modes is negligible [5], [8].

Now, from the orthogonality property of the spherical vector harmonics we obtain that the total available power is given by

$$\begin{aligned} P_E &= \frac{1}{4}\langle\|\boldsymbol{f}\|^2\rangle = \frac{1}{4}\mathrm{tr}(\boldsymbol{\mathcal{R}}_f) \\ &= \sum_{\iota=1}^{\infty} P_\iota^{\text{pol}} + P_\iota^{\text{unpol}}, \end{aligned} \tag{3.15}$$

where $P_E = P_{\text{pol}} + P_{\text{unpol}}$. The factor 4 is introduced to take into account that f is obtained for regular waves, while we are only interested in the power of the incoming waves.

We can further normalize the total field power to the unity[5], $P_E = 1$, and then we can rewrite the relative mode power in the following way

$$P_\iota = \frac{P_\iota^{\text{pol}} + P_\iota^{\text{unpol}}}{P_{\text{pol}} + P_{\text{unpol}}}. \tag{3.16}$$

Hence, after some algebraic manipulations the mode power can be expressed as

$$\begin{aligned} P_\iota &= \frac{4\pi}{1+\chi}\int \frac{\chi\left|A_{\iota,\theta}(\Omega)\right|^2 p_\theta(\Omega)}{1+K_\theta} \\ &\quad + \frac{\left|A_{\iota,\phi}(\Omega)\right|^2 p_\phi(\Omega)}{1+K_\phi}\mathrm{d}\Omega \\ &\quad + \frac{4\pi}{1+\chi}\left(\sqrt{\frac{\chi K_\theta}{1+K_\theta}}\left|A_{\iota,\theta}(\Omega_0)\right| + \sqrt{\frac{K_\phi}{1+K_\phi}}\left|A_{\iota,\phi}(\Omega_0)\right|\right)^2. \end{aligned} \tag{3.17}$$

Equation (3.17) corresponds to the mean effective gain (MEG) [2], with the difference that instead of the partial gains we have the absolute values of the components of the spherical vector harmonics, $4\pi\left|A_{\iota,\theta}\right|^2$ and $4\pi\left|A_{\iota,\phi}\right|^2$, respectively. The physical meaning of the mode power in a Gaussian field becomes apparent. Indeed,

[5] Here it is important to observe the normalization of the total multi-pole power, $\sum_{\tau=1}^{2}\sum_{m=-l}^{l}\sum_{l=1}^{L} P_{\tau ml} = \frac{L(L+2)}{4\pi}$,which directly follows from the addition theorem of spherical vector waves in Appendix A.

the mode power corresponds to the mode "link gain" between the multi-poles and the source to the incoming field. Hence, by exciting the appropriate modes the quality of the communication link is maximized.

4 Scattering matrix of an antenna and optimal antenna communication performance in fading channels

In the previous section we showed that the expansion coefficients into spherical vector waves are also Gaussian variates as a result of the model used for the incident field. In this section we present the link between the incident field and the antenna with the purpose of investigating its properties in random fields.

All of the properties of an N-port antenna as transmitting, receiving or scattering device are contained in the scattering matrix [15]. The scattering matrix of an antenna relates the incoming signals, $\boldsymbol{v}$ and waves, $\boldsymbol{a}$, with the outgoing signals, $\boldsymbol{w}$ and waves $\boldsymbol{b}$. The scattering matrix is given by

$$\begin{pmatrix} \mathbf{\Gamma}^{N\times N} & \mathbf{R}^{N\times\infty} \\ \mathbf{T}^{\infty\times N} & \mathbf{S}^{\infty\times\infty} \end{pmatrix} \begin{pmatrix} \boldsymbol{v}^{N\times 1} \\ \boldsymbol{a}^{\infty\times 1} \end{pmatrix} = \begin{pmatrix} \boldsymbol{w}^{N\times 1} \\ \boldsymbol{b}^{\infty\times 1} \end{pmatrix}, \tag{4.1}$$

where $\mathbf{\Gamma}$ is the matrix containing the complex antenna reflection coefficients, $\mathbf{R}$ is the matrix containing the antenna receiving coefficients, $\mathbf{T}$ is the matrix containing the antenna transmitting coefficients and $\mathbf{S}$ is the matrix containing the antenna scattering coefficients.

The total electric field associated with the antenna is here expanded in incoming, $\mathbf{u}^{(1)}_{\tau ml}(k\boldsymbol{r})$, and outgoing, $\mathbf{u}^{(2)}_{\tau ml}(k\boldsymbol{r})$, spherical vector waves or modes [15]

$$\boldsymbol{E} = k\sqrt{2\eta}\sum_{l=1}^{\infty}\sum_{m=-l}^{l}\sum_{\tau=1}^{2} a_{\tau ml}\mathbf{u}^{(1)}_{\tau ml}(k\boldsymbol{r}) + b_{\tau ml}\mathbf{u}^{(2)}_{\tau ml}(k\boldsymbol{r}), \tag{4.2}$$

where $a_{\tau ml}$ (incoming waves $\boldsymbol{a}$) and $b_{\tau ml}$ (outgoing waves $\boldsymbol{b}$) are the corresponding multipole coefficients. A brief description of the spherical vector waves is given in Appendix A.

In order to analyze the interaction of the antenna with a random propagation channel we first determine the transmission matrix as a projection of the far-field of the antenna on the spherical vector harmonics, $\boldsymbol{A}_{\tau ml}$, in transmitting regime. Hence, the far-field $\boldsymbol{F}_n(\hat{\boldsymbol{r}})$ of port n is given by

$$\boldsymbol{F}_n(\hat{\boldsymbol{r}}) = k\sqrt{2\eta}\sum_{l=1}^{\infty}\sum_{m=-l}^{l}\sum_{\tau=1}^{2} \mathrm{i}^{l+2-\tau} T_{\tau ml,n}\boldsymbol{A}_{\tau ml}(\hat{\boldsymbol{r}})v_n, \tag{4.3}$$

where $\boldsymbol{A}_{\tau ml}(\hat{\boldsymbol{r}})$ is defined in Appendix A, $\hat{\boldsymbol{r}}$ is the unitary spatial coordinate and v_n is the signal incident on port n with corresponding power normalization, $\|\boldsymbol{v}\|^2 = 1$.

Further, applying the orthogonality properties of spherical vector harmonics, we obtain the transmission coefficients of the antenna

$$T_{\tau ml,n}v_n = \frac{\mathrm{i}^{-l-2+\tau}}{k\sqrt{2\eta}} \int \boldsymbol{A}^*_{\tau ml}(\hat{\boldsymbol{r}}) \cdot \boldsymbol{F}_n(\hat{\boldsymbol{r}}) \mathrm{d}\Omega. \tag{4.4}$$

Evoking the Lorentz reciprocity theorem we arrive at the matrix containing the receiving coefficients [15]

$$R_{n,\tau ml} = (-1)^m T_{\tau(-m)l,n}. \tag{4.5}$$

Since we are interested in the receiving regime we set, $\boldsymbol{v} = \mathbf{0}$ for the incoming signals. Then, from the scattering matrix we can now infer the relationship between the outgoing signals and the incoming waves for a lossless N-port antenna

$$\boldsymbol{w} = \mathbf{R}\boldsymbol{a}, \tag{4.6}$$

where $\boldsymbol{a}$, is a vector containing the expansion coefficients of incoming waves.

It is worthwhile to note that, even if the treatment focuses on the receiver regime of the antenna, the exposed theory applies also to the transmission regime due to the reciprocity conditions (4.5). Furthermore, in the previous sections we studied the spherical vector wave expansion of Gaussian fields, more exactly we studied the model of the superposition of plane waves for the incident field at a spherical volume. The expansion coefficients a_ι, are related to the expansion coefficients f_ι, of regular waves, with multipole index ι, as $2a_\iota = f_\iota$, and therefore $P_E = \|\boldsymbol{a}\|^2_F = \frac{1}{4}\|\boldsymbol{f}\|^2_F$. This result follows from the properties of the spherical vector wave functions and the fact that the outgoing an incoming waves carry the same power in free space (empty minimal sphere), i.e., $\|\boldsymbol{a}\|^2_F = \|\boldsymbol{b}\|^2_F$, where the scattering matrix $\mathbf{S} = \mathbf{I}$.

Expressions (4.3)-(4.6) can readily be used for the analysis of the interaction between an N-port antenna system with the far-field radiation patterns, $\boldsymbol{F}_n(\hat{\boldsymbol{r}})$ and a random propagation channel denoted by $\boldsymbol{a}$. These relationships enable the evaluation of communication performance of multiple antennas in a given propagation channel. Also, they constitute a tool for evaluating communication performance bounds of generic antennas in the context of Gaussian channels as we will show in Section 4. A.

The scattering matrix formalism is valid for any signals $\boldsymbol{w}$, $\boldsymbol{v}$ and waves $\boldsymbol{a}$, $\boldsymbol{b}$, including waves that can be modelled by random variables, while the antenna matrices $\mathbf{\Gamma}$, $\mathbf{R}$, $\mathbf{T}$ and $\mathbf{S}$ are deterministic in general. In the following we show some results applicable for general propagation channels and antennas modelled by the scattering matrix.

Next we present some results for optimal antennas in a general channel but also in multimode Gaussian channels described in Sec. 3. We are looking at the link communication performance of an antenna in Gaussian field generated by a transmitting device, which has propagated through the channel. We assume that the receiving and transmitting antennas are separated at a sufficient distance so that no mutual coupling occurs. We analyze both the total link power and the cross-correlation between signal received at different antenna ports.

4.1 Maximum received power

In wireless communications the link quality is of great importance for the successful transmission of information. Link quality is directly connected to link gain, which in turn, among other parameters, depends on path gain, antenna characteristics and transmitted power. The following proposition summarizes the general conditions under which we can increase link communication power in terms of transmission and reception coefficients of field multimodes.

Proposition 2. *The optimal "instantaneous" power of the outgoing signals,* $\|\boldsymbol{w}\|^2$*, of an N-port antenna in a random field,* $\boldsymbol{a}$*, is*

$$\max \|\boldsymbol{w}\|_F^2 = 4\pi \sum_{n=1}^{N} \eta_n \|\boldsymbol{a}\|_F^2 . \tag{4.7}$$

The optimal value is achieved for matched transmission (reception) coefficients,

$$R_{n,\iota} = \sqrt{4\pi\eta_n} \mathrm{e}^{\mathrm{i}\varphi_n} \frac{a_\iota^*}{\|\boldsymbol{a}\|_F}, \tag{4.8}$$

where η_n *is the radiation efficiency of port* n *and* φ_n *is an arbitrary phase. The derivation is given in Appendix D.*□

The physical interpretation is straightforward: the received power (or similarly the transmitted power due to reciprocity) is maximized if the incoming (outgoing) waves are conjugate matched by the receiver (transmitter) coefficients. This of course requires the knowledge of each realization of the incoming field. It is worthwhile to notice that in practice, when a specific geometry, physically realizable materials and matching networks are considered, the number of multimodes that could possibly be excited is not arbitrary. As we mentioned earlier, higher modes will suffer from losses that depend on the ratio between the radius of the minimum sphere enclosing the antenna to the radiation wavelength. Hence, for electrically small antennas only low order multipoles are of interest [5], [12].

Proposition 3. *The average of the optimal power of the outgoing signals,* $\|\boldsymbol{w}\|^2$*, of an N-port antenna in a random field,* $\boldsymbol{a}$ *is*

$$\langle \max \|\boldsymbol{w}\|_F^2 \rangle = 4\pi \langle \|\boldsymbol{a}\|_F^2 \rangle \sum_{n=1}^{N} \eta_n = 4\pi P_E \sum_{n=1}^{N} \eta_n . \tag{4.9}$$

This result follows directly from Proposition 2.□

Equation (4.9) gives the average of the maximized received power, which is in general different from the maximum average power, i.e., $\langle \max \|\boldsymbol{w}\|_F^2 \rangle \neq \max \langle \|\boldsymbol{w}\|_F^2 \rangle$.

In many practical situations we would like to assess the communication performance of antennas, or in general any radiating device, in actual multipath propagation channels, e.g., testing the communication performance of mobile handsets in wireless networks. A parameter that actually takes into account both the antenna and the channel is the MEG [27]. Here, we present a definition based on the spherical vector wave expansion.

Definition 4.1. *Let an antenna be described by the scattering matrix* (4.1)*, then we define the Mean Effective Gain (MEG) of the antenna as the ratio of the average power of the outgoing signals,* $\langle \|\boldsymbol{w}\|_F^2 \rangle$*, to the average power of the incoming waves,* $\langle \|\boldsymbol{a}\|_F^2 \rangle$

$$G_{\mathrm{e}} = \frac{\langle \|\boldsymbol{w}\|_F^2 \rangle}{\langle \|\boldsymbol{a}\|_F^2 \rangle}. \tag{4.10}$$

□

Proposition 4. *The MEG of an* N*-port antenna in a random field,* $\boldsymbol{a}$*, is upper bounded by*

$$G_{\mathrm{e}} \leq 4\pi \sum_{n=1}^{N} \eta_n, \tag{4.11}$$

where equality is achieved by conjugate mode matching. The result follows directly from Proposition 3.□

This result corroborates a similar result shown in [2].

4.2 Minimum correlation

In the previous section we studied the conditions that provide maximum power for the output waves. In this section we instead focus on the cross-correlation characteristics of the output waves.

Consider the following correlation definition

$$\boldsymbol{\mathcal{R}}_w = \mathbf{R}\boldsymbol{\mathcal{R}}_a\mathbf{R}^H, \tag{4.12}$$

where $\boldsymbol{\mathcal{R}}_w = \langle \boldsymbol{w}\boldsymbol{w}^H \rangle$ is the correlation matrix of outgoing waves of dimensions $N \times N$ and $\boldsymbol{\mathcal{R}}_a = \langle \boldsymbol{a}\boldsymbol{a}^H \rangle$ is the mode correlation with dimensions $\infty \times \infty$.

It is known that in order to maximize the diversity gain of a system with multiples antennas, the received signals, $\boldsymbol{w}$, at the different antenna ports, should be uncorrelated [21]. Hence, $\boldsymbol{\mathcal{R}}_w$ must be diagonal. Proposition 5 summarizes the general conditions under which we can achieve this diagonalization.

Proposition 5. *The correlation matrix of the outgoing signals,* $\boldsymbol{w}$*, of an* N*-port antenna in a random field,* $\boldsymbol{a}$*, is diagonalized as,*

$$\boldsymbol{\mathcal{R}}_w = \frac{4\pi}{N}\boldsymbol{\Lambda}_{a,N} \sum_{n=1}^{N} \eta_n, \tag{4.13}$$

by the reception matrix,

$$\mathbf{R} = \mathrm{e}^{\mathrm{i}\varphi} \left(\frac{4\pi}{N} \sum_{n=1}^{N} \eta_n \right)^{\frac{1}{2}} \mathbf{U}_{a,N}^H, \tag{4.14}$$

where $\boldsymbol{\Lambda}_{a,N}$ *is diagonal matrix containing the* N *strongest and distinct eigenvalues of* $\boldsymbol{\mathcal{R}}_a$*, and* $\mathbf{U}_{a,N}$ *is the matrix containing the corresponding eigenvectors. The derivation is given in Appendix E.*□

The physical interpretation of Proposition 8 is that in order to diagonalize the correlation matrix of the received signals, $\boldsymbol{\mathcal{R}}_w$, and at the same time obtain the largest possible power, then the columns of the receiving matrix $\mathbf{R}$ should be chosen so that they equal the eigenvectors of the matrix $\boldsymbol{\mathcal{R}}_a$ corresponding to its N strongest and distinct eigenvalues.

Remark 2. *The received power of the minimum correlation N-port antenna in a random field, $\boldsymbol{a}$, is therefore*

$$\langle \|\boldsymbol{w}\|_F^2 \rangle = \frac{4\pi}{N} \sum_{n=1}^{N} \eta_n \mathrm{tr} \mathbf{\Lambda}_{a,N}. \tag{4.15}$$

□

5 Numerical examples

It is well understood that the same antenna performs differently depending on the operating environment, i.e., an antenna that is good in one propagation environments might not operate equally well in other environments. Therefore, knowing the properties of the propagation channel is indispensable if communication performance is to be optimized. In this context, channel modelling naturally becomes an important link in the antenna design process. In general, channel modeling is a wide field of research and realistic channel models can be quite complex, see e.g., [27], [3], [7]. However, since we here just aim at illustrating the role of spatio-polar selectivity in the antenna-channel interaction we are going to present simulation results based on a simple channel model where a two dimensional Laplacian distribution in spherical coordinates is assumed for the AoA for each of the two orthogonal polarizations, i.e.,

$$p_{\theta,\phi\mathrm{x}}(\theta,\phi) = p_{\theta\mathrm{x}}(\theta) p_{\phi\mathrm{x}}(\phi) = A \mathrm{e}^{-\frac{\sqrt{2}|\theta-\mu_\theta|}{\sigma_\theta} - \frac{\sqrt{2}\left|\phi-\mu_\phi\right|}{\sigma_\phi}} \sin\theta, \tag{5.1}$$

where $\theta \in [0,\pi]$, $\phi \in [0, 2\pi)$ and x stands for either of $\hat{\boldsymbol{\theta}}$ or $\hat{\boldsymbol{\phi}}$, polarization, and the shape is controlled by the distribution parameters $\{\mu_{\theta\mathrm{x}}, \sigma_{\theta\mathrm{x}}, \mu_{\phi\mathrm{x}}, \sigma_{\phi\mathrm{x}}\}$. The XPR expressed in dB takes on three values, i.e., $\chi \in [-10, 0, 10]$, which is approximately the span of variation of the XPR of the incident field measured in cellular communication channels. Further, in order to simplify the analysis we assume that $\sigma = \sigma_{\theta\mathrm{x}} = \sigma_{\phi\mathrm{x}} \in [0.1, 1, 10]$. It is worthwhile to observe that the isotropic model is obtained as a limit case of the 2D Laplacian model (5.1) by letting, $\sigma_{\theta\mathrm{x}}, \sigma_{\phi\mathrm{x}} \to \infty$,

$$p_{\theta,\phi}(\theta,\phi) = \frac{\sin\theta}{4\pi}, \theta \in [0,\pi], \phi \in [0, 2\pi). \tag{5.2}$$

Moreover, with the isotropic AoA distribution, a zero dB channel XPR is usually assumed, i.e. $\chi = 0\mathrm{dB}$, meaning that the power in the two orthogonal polarizations is the same. The presented models produce a Rayleigh probability density function for the envelopes of the received signals.

5.1 The rectangular microstrip element in a Gaussian field with Laplacian PAS

The rectangular microstrip element or patch antenna is a good example of an antenna widely used in many applications due to its versatility, e.g., in terms of diversity of patterns and polarizations. Here, we use a numerical model of a probe fed patch antenna on a dielectric substrate simulated with the efield electromagnetic solver [1]. The coaxial probe is modelled by a wire with a delta voltage source. All parts are centered at the origin of a right handed Cartesian coordinate system. The geometrical parameters of the antenna are as follows: length $L = 30$ mm, width $W = 18$ mm and feed position from center, $D = 4$ mm. The square ground plane is of dimension $L_g = 60$ mm, the substrate thickness is $T = 3$ mm with relative dielectric constant $\varepsilon = 2.0$. The antenna resonance frequency is 3.25 GHz. We consider two different orientations of the patch: in the first, the antenna substrate is on the horizontal, x-y plane; in the second the substrate is vertically oriented (obtained by rotating the z-axis towards the x-axis), which we denote as horizontal patch and vertical patch, respectively.

The spherical vector wave mode expansion coefficients of the horizontal patch and vertical patch antennas are given in Fig. 2 a) and b), respectively. Observe that only the mode indices excited by the antennas are shown. As can be seen the multi-pole modes that are predominantly excited by the patch antennas are the dipole moments with multi-indices from 1 to 6.

The corresponding average powers of the modes excited by the random field generated accordingly to the Laplacian probability density functions (5.1) are shown in Fig. 3. At first glance the behavior of the modes seems rather “chaotic", however, a closer look reveals a systematic behavior as predicted by the theory provided in previous sections. Several observations follow from the plots in Fig. 3. Firstly, we can observe that the powers of the different modes become more uniform as the r.m.s. angle spread, σ, increases, i.e., the channel becomes less selective in the multi-mode domain. This is a consequence of the well-known fact that the more uniform the distribution of AoAs on the sphere of unit radius, the smaller the significance of particular orientation in space. Secondly, the average mode powers show a symmetric dependence in the τ index as a function of the channel cross-polarization ratio, χ when expressed in dB. For example, compare plots a), d) and g): as χ changes from -10 dB to 10 dB, the power of the TE modes ($\tau = 1$) and TM modes ($\tau = 2$) interchange values for fixed m and l indices. Thus, the dipole mode with $\iota = 1$ for $\chi = -10$ dB has the same power as the dipole mode with $\iota = 2$ for $\chi = 10$ dB and vice-versa, while for $\chi = 0$ dB both powers are equal. The same applies for dipole pairs 3 and 4 and 5 and 6, etc. Hence, selectivity/non-selectivity in the spatio-polar domain is equivalent to the selectivity/non-selective in the mode domain.

In Section 4 we gave a definition of the MEG in terms of the spherical vector wave expansion coefficients. As we stated there, the MEG is a figure of merit of the interaction of the antenna with the channel. The physical meaning is straightforward, the more multimodes excited by the antenna match the corresponding

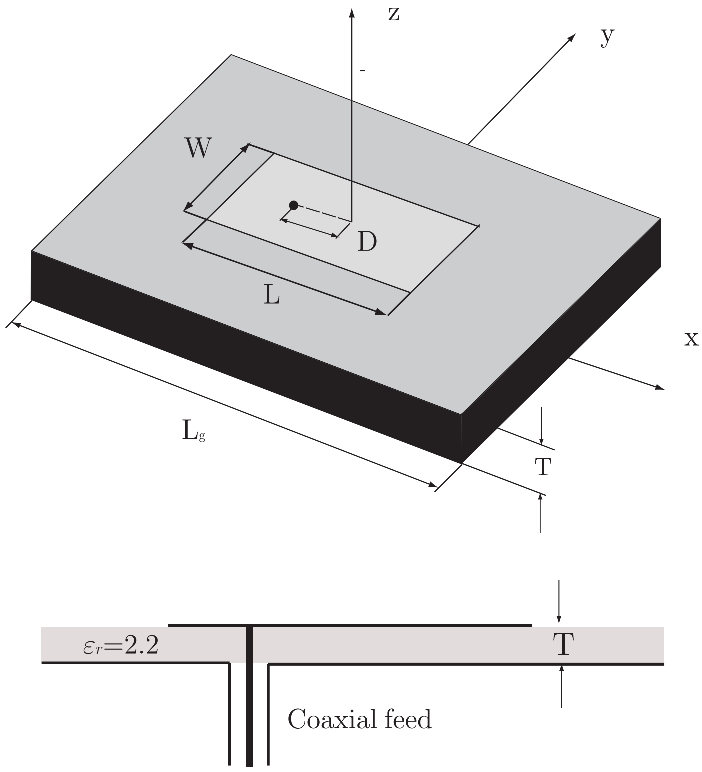

Figure 1: The horizontal patch antenna. The vertical patch is obtained by a rotation around the y-axis towards the x-axis

channel modes, the better the antenna performance will be in terms of link gain. This is illustrated in Fig. 4, where the cdf (cumulative distribution function) of the normalized "instantaneous" link gain[6] $G_{\mathrm{i}} = \frac{\|\boldsymbol{w}\|_F^2}{\langle\|\boldsymbol{a}\|_F^2\rangle}$, is shown. Curves for the horizontally oriented patch and the vertically oriented patch antennas are represented by the discontinuous and continuous lines, respectively. As can be seen the MEG is different for all the 9 propagation scenarios considered. This can be explained by the fact that the directivity of the two considered antennas have not been suitably matched to the PAS of the incoming field. Or looking at it from the point of view of the spherical vector waves, the multimodes excited by the antenna (Fig. 2) do not match the corresponding channel multimodes (Fig. 3). In general, for some channel realizations the "matching" is bad, while for others it is much better, which gives place to the "fading" behavior. The dynamic range varies between 20 to 40 dB.

Also in Section 4 we showed the conditions for link gain maximization: multimode conjugate mode matching, (4.11). An example of the conjugate mode matching for idealized antennas is given which is illustrated in Fig. 3. The plots depict the "instantaneous" link gain of antennas that are mode-matched only to the TM dipole modes. Here we can see that even if the MEG in this case does not equal $10\log_{10}(4\pi) \approx 11$dB as it would be obtained by the full mode matching, a con-

[6]We assume 100 % efficient antennas, i.e., $\eta_n = 1$ for all n antenna ports.

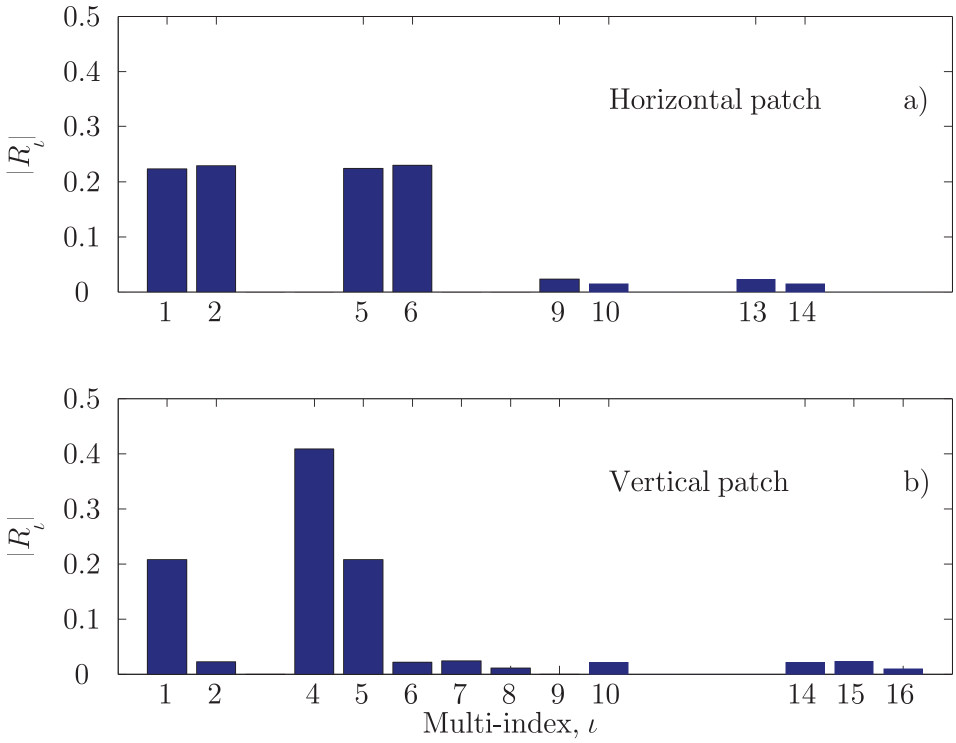

Figure 2: Spherical vector wave expansion coefficients of a) horizontal patch antenna and b) the vertical patch antenna.

siderable increase in performance is observed and it is independent from the channel cross-polarization ratio, χ and only slightly dependent on the angle spread, σ. This immediately suggests that, in principle, if an antenna is constructed such as it conjugate-matches the three lowest dipoles a considerable link power improved could be obtained in most cases compared with the two patches.

5.2 The elementary "Tripole" in a Gaussian field with Laplacian PAS

Here, we have chosen to investigate the spatio-polar performance of antennas by means of the "tripole" antenna [6]. The main reason for choosing this antenna is that it combines the three lowest modes of the electromagnetic field but still might provide full polarization flexibility as we saw from the previous section. The tripole antenna is a polarization diversity antenna system.

Fig. 5 shows the statistics of the normalized squared envelope corresponding to the three-orthogonal dipoles that correspond to the first three electrical modes of the multi-pole expansion, $|f_\iota|^2$, with $\iota = 2$ corresponding to the multi-index set $\{2, -1, 1\}$, $\iota = 6$ to $\{2, 1, 1\}$ and $\iota = 4$ to $\{2, 0, 1\}$,respectively, where the multi–index ι, is ordered and identified with the number $\iota = 2(l^2 + l - 1 + m) + \tau$. Cumulative distribution functions (cdf) of the three polarization branches of the tripole antenna

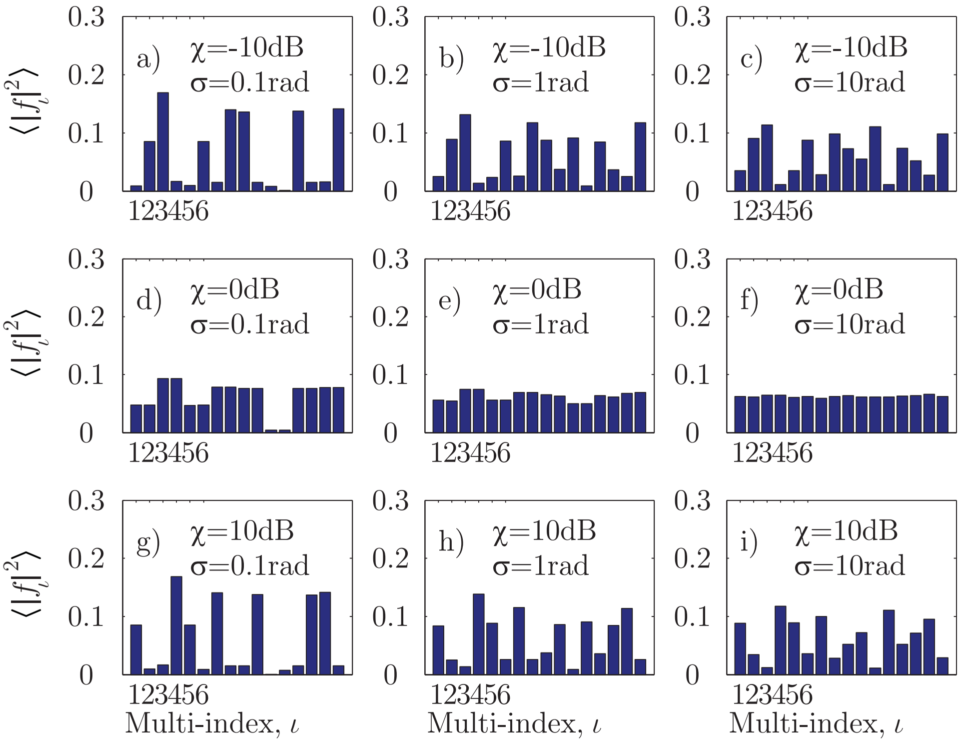

Figure 3: Average mode power versus mode index for the random field simulated according to (5.1).

are shown for different values of the channel cross-polarization ratio, χ and the σ-parameter of the Laplace distribution of the AoA. Observe that, as expected, the powers of the two horizontal dipoles, $|f_2|^2$ and $|f_6|^2$ are identically distributed, while the power of the vertical dipole, $|f_4|^2$, (depicted by the discontinuous line) is shifted some dBs to the left or the right depending on the channel XPR.

From a closer analysis of Fig. 5, we see that the average power of the three modes satisfies the following inequalities at all angle spread values σ,

$$\langle|f_2|^2\rangle = \langle|f_6|^2\rangle > \langle|f_4|^2\rangle, \text{ for } \chi = -10\text{dB} \tag{5.3}$$

$$\langle|f_2|^2\rangle = \langle|f_6|^2\rangle \simeq \langle|f_4|^2\rangle, \text{ for } \chi = 0\text{dB} \tag{5.4}$$

$$\langle|f_2|^2\rangle = \langle|f_6|^2\rangle < \langle|f_4|^2\rangle, \text{ for } \chi = 10\text{dB}. \tag{5.5}$$

This is a result of power imbalance between the $\hat{\boldsymbol{\theta}}$ and $\hat{\boldsymbol{\phi}}$ polarizations, quantified by the channel XPR, χ, even when the total field is unpolarized as it is the case in our simulations. Hence, in this type of channels, the polarization imbalance has a larger impact on the mode power than the angle spread. On the other hand, the angle spread has a major impact on the correlation of the different multimodes. Fig. 5 shows the elements of the correlation matrix $R_{\iota'\iota}$.

Here we can observe that mode correlation increases for low angular spreads, while it decreases for more isotropic channels. This, of course, is a known result.

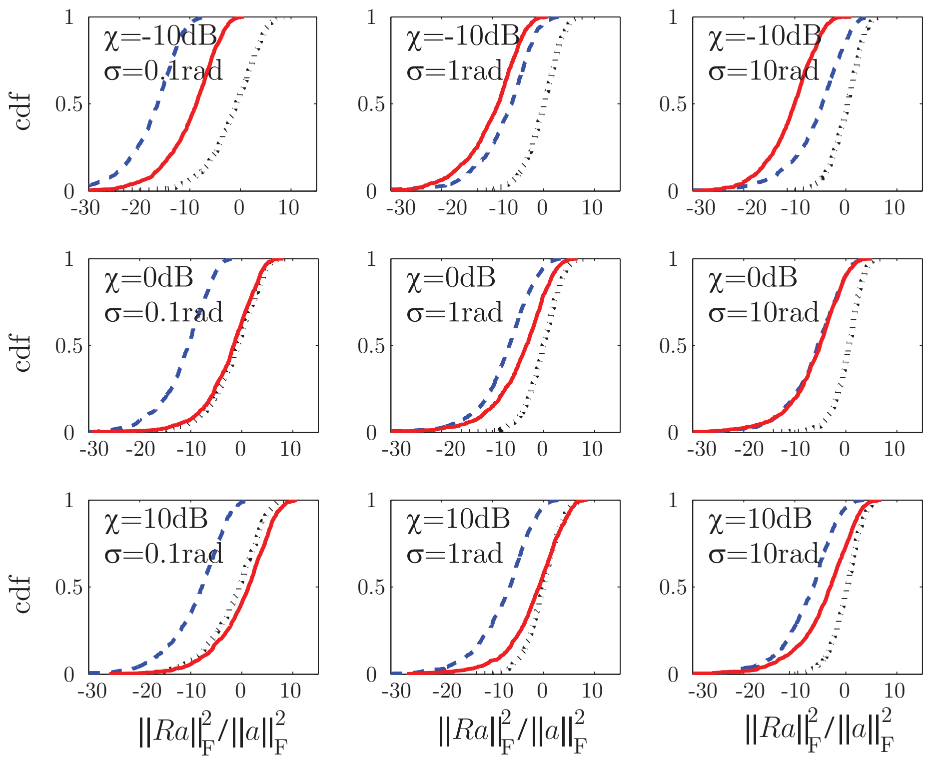

Figure 4: Cumulative distribution functions (cdf) of the normalized instantaneous gain of the horizontal patch (−−), the vertical patch (−) and the conjugate matched antennas, $(\cdots)$. Results are shown for different values of the channel cross-polarization ratio, χ and the σ-parameter of the Laplace distribution of the AoA.

However, the new aspect here is that we can achieve uncorrelated signals based on the mode analysis of the channel as shown in Section 4. Here, we have limited our analysis to the three lowest modes for illustrative purposes only. In general (as shown in Section 4) the degrees of freedom for diversity and spatial multiplexing transmission are limited by the minimum of the number of excited modes and the number of antenna ports.

Since we have three modes that can be excited at three antenna ports, the solution to decorrelated signal is given by (4.14), which states that the transmission matrix should be equal to the Hermitian transpose of the matrix containing the eigenvectors of the correlation matrix of the multi-poles. By doing so we indeed achieve uncorrelated signals. The fading variation of the combined antenna diversity branches is identical to the Maximum Ratio Combining (MRC) applied to the multi-poles. The cdf of the MRC signal is shown in Fig. 6 and is identical to the cdf of TM-2 matched signal, i.e., in this case mode matching and MRC are equivalent.

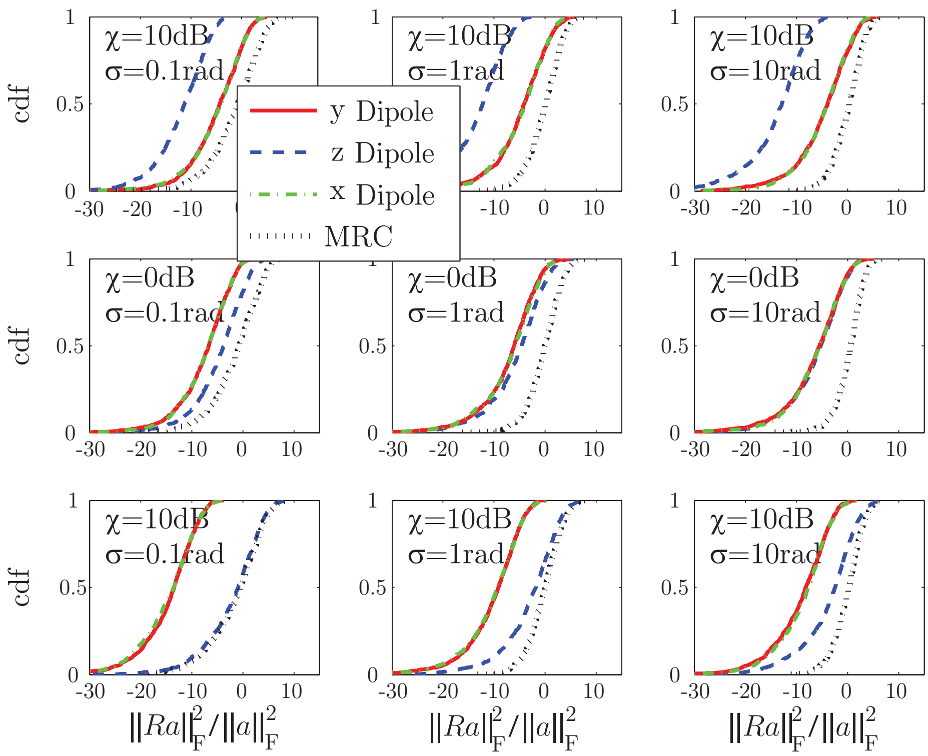

Figure 5: Cumulative distribution functions (cdf) of w of the vertical dipole and the two horizontal dipole elements of the tripole antenna denoted by $(--)$, $(-\ )$ and $(\ \cdot - \cdot -)$, respectively. Results are shown for different values of the channel cross-polarization ratio, χ and the σ-parameter of the Laplace distribution of the AoA, where $\iota = \{\tau m l\}$ is the multi-pole multi-index.

6 Summary

In this paper we have introduced a new approach to analyze the interaction between antennas and the propagation channel. Our method employs the scattering matrix of the antenna and the spherical vector wave expansion of the electromagnetic field. The focus is on the spatio-polar characterization of the antennas, the channel and their interaction. The key contribution of our paper can be summarized as follows: we show that in a Gaussian electromagnetic field (the propagation channel) each multimode coefficient in the spherical vector wave expansion is a Gaussian variate, as a consequence the envelope of each multimode coefficient in the spherical vector wave expansion is a Ricean variate. We derive closed-form expressions for the mode correlation matrix for arbitrary power angular spectra (PAS) of incoming waves, we derive closed-form expressions for the normalized power of single modes in terms of the PAS of incoming waves and the channel cross-polarization ratio (XPR). We then show that maximum received (transmitted) power is achieved by conjugate mode matching and that independent signals are achieved by eigenmode (reception) transmission over the strongest multimodes. A definition of the MEG of antennas

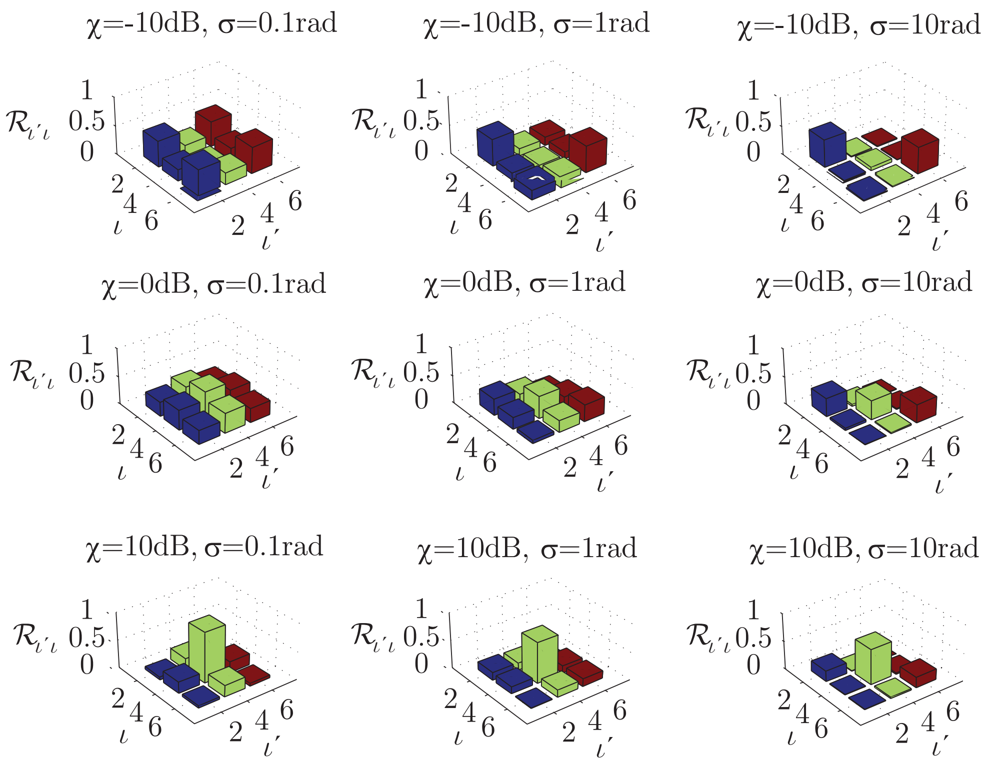

Figure 6: Elements of the covariance matrix $R_{\iota'\iota}$ where $\iota = \{\tau m l\}$ is the multi-pole multi-index where $2 = \{2, -1, 1\}$, $4 = \{2, 0, 1\}$ and $6 = \{2, 1, 1\}$.

based on scattering matrix parameters is provided and we show that maximum MEG is achieved by conjugate mode matching. The results presented here provide not only limits on the achievable performance of antennas in random propagation channels, but also provide a framework for a detailed analysis of antenna-channel interaction. Future work will investigate MIMO systems and whether this framework can also be used for antenna synthesis.

Acknowledgments

This work has been supported by SSF High Speed Wireless Center and an INGVAR grant from the Swedish Foundation for Strategic Research. We thank the anonymous reviewers for their valuable suggestions that greatly helped to improve the paper.

Appendix A. Spherical vector waves

The regular spherical vector waves are given by

$$\mathbf{v}_{1ml}(k\boldsymbol{r}) = \mathrm{j}_l(kr)\mathbf{A}_{1ml}(k\hat{\boldsymbol{r}}), \tag{6.1}$$

$$\begin{aligned}\mathbf{v}_{2ml}(k\boldsymbol{r}) &= \frac{(kr\mathrm{j}_l(kr))'}{kr}\mathbf{A}_{2ml}(k\hat{\boldsymbol{r}}) \\ &\quad+\sqrt{l(l+1)}\frac{\mathrm{j}_l(kr)}{kr}\mathbf{A}_{3ml}(k\hat{\boldsymbol{r}}),\end{aligned} \tag{6.2}$$

where the time convention $\mathrm{e}^{\mathrm{i}\omega t}$ is used and $\mathrm{j}_l(kr)$ are the regular spherical Bessel functions.

Similarly, the incoming ($p = 1$) and outgoing ($p = 2$) spherical vector waves, $\mathbf{u}^{(p)}_{\tau ml}(k\boldsymbol{r})$ are given by

$$\mathbf{u}^{(p)}_{1ml}(k\boldsymbol{r}) = \mathrm{h}^{(p)}_l(kr)\mathbf{A}_{1ml}(k\hat{\boldsymbol{r}}), \tag{6.3}$$

$$\begin{aligned}\mathbf{u}^{(p)}_{2ml}(k\boldsymbol{r}) &= \frac{(kr\mathrm{h}^{(p)}_l(kr))'}{kr}\mathbf{A}_{2ml}(k\hat{\boldsymbol{r}}) \\ &\quad+\sqrt{l(l+1)}\frac{\mathrm{h}^{(p)}_l(kr)}{kr}\mathbf{A}_{3ml}(k\hat{\boldsymbol{r}}),\end{aligned} \tag{6.4}$$

where $\mathrm{h}^{(p)}_l(kr)$ are the spherical Hankel functions of the p-th kind.

The functions $\mathbf{A}_{\tau ml}(k\hat{\boldsymbol{r}})$ are the spherical vector harmonics that satisfy the complex valued inner product, i.e. orthogonality on the unit sphere [15],

$$\int \mathbf{A}_{\tau ml}(\hat{\boldsymbol{r}}) \cdot \mathbf{A}^*_{\tau' m' l'}(\hat{\boldsymbol{r}})\mathrm{d}\Omega = \delta_{\tau\tau'}\delta_{mm'}\delta_{ll'}. \tag{6.5}$$

The addition theorem for the vector spherical harmonics is

$$\sum_{m=-l}^{l} \mathbf{A}_{\tau ml}(\hat{\boldsymbol{r}}) \cdot \mathbf{A}^*_{\tau' m' l'}(\hat{\boldsymbol{r}})\mathrm{d}\Omega = \frac{2l+1}{4\pi} \tag{6.6}$$

Appendix B. Proof of Proposition 1

Proof. The correlation matrix for the expansion coefficients, i.e., mode correlation is computed as

$$\mathcal{R}_{\iota\iota'} = \langle f^*_\iota f_{\iota'}\rangle. \tag{6.7}$$

Now, in order to simplify the notation we use the integral representation obtained in the limiting case of a continuum of incoming waves. Hence, the coefficients can be computed as

$$f_\iota = \frac{4\pi(-\mathrm{i})^{l-\tau+1}}{k\sqrt{2\eta}} \int \boldsymbol{E}_0(\hat{\boldsymbol{k}}) \cdot \boldsymbol{A}^*_\iota(\hat{\boldsymbol{k}})\mathrm{d}\Omega, \tag{6.8}$$

Hence,

$$
\begin{aligned}
\mathcal{R}_{\iota\iota'} &= \frac{8\pi^2(-\mathrm{i})^{l-l'-\tau+\tau'}}{\eta k^2}\dots \\
&\quad \dots\int\int\langle \boldsymbol{E}_0\cdot\boldsymbol{A}^*_{\iota}\boldsymbol{E}'^*_0\cdot\boldsymbol{A}'_{\iota'}\rangle\mathrm{d}\Omega\mathrm{d}\Omega' \\
&= \frac{8\pi^2(-\mathrm{i})^{l-l'-\tau+\tau'}}{\eta k^2}\dots \\
&\quad \dots\int\int\langle E_\theta E'^*_\theta\rangle A^*_{\iota,\theta}A'_{\iota',\theta} \\
&\quad +\langle E_\theta E'^*_\phi\rangle A^*_{\iota,\theta}A'_{\iota',\phi} \\
&\quad +\langle E_\phi E'^*_\theta\rangle A^*_{\iota,\phi}A'_{\iota',\theta} \\
&\quad +\langle E_\phi E'^*_\phi\rangle A^*_{\iota,\phi}A'_{\iota',\phi}\mathrm{d}\Omega\mathrm{d}\Omega',
\end{aligned}
\tag{6.9}
$$

Further, by inserting the spatial correlation conditions (2.4) we obtain that the mode correlation can be expressed as the sum of the mode correlation corresponding to the polarized and the unpolarized components

$$
\mathcal{R}_{\iota\iota'} = \mathcal{R}^{\mathrm{pol}}_{\iota\iota'} + \mathcal{R}^{\mathrm{unpol}}_{\iota\iota'},
\tag{6.10}
$$

where mode correlation of the polarized component is given by

$$
\begin{aligned}
\mathcal{R}^{\mathrm{pol}}_{\iota\iota'} &= 4\pi(-\mathrm{i})^{l-l'-\tau+\tau'}(P_{0\theta}A^*_{\iota,\theta}(\Omega_0)A_{\iota',\theta}(\Omega_0) \\
&\quad +2\,\mathrm{Re}\left\{\sqrt{P_{0\theta}P_{0\phi}}A^*_{\iota,\theta}(\Omega_0)A_{\iota',\phi}(\Omega_0)\mathrm{e}^{\mathrm{i}\psi}\right\} \\
&\quad +P_{0\phi}A^*_{\iota\phi}(\Omega_0)A_{\iota',\phi}(\Omega_0)),
\end{aligned}
\tag{6.11}
$$

where $\sqrt{P_{0\theta}P_{0\phi}} = \frac{2\pi}{\eta k^2}\left|E_\theta E^*_\phi\right|$ and ψ is a phase angle that depends on the polarization, e.g., $\psi = 0$, for a linearly polarized wave and $\psi = \pm\frac{\pi}{2}$for circularly polarized waves. Similarly, the mode correlation corresponding to the unpolarized component can be calculated as follows

$$
\begin{aligned}
\mathcal{R}^{\mathrm{unpol}}_{\iota\iota'} &= 4\pi(-\mathrm{i})^{l-l'-\tau+\tau'}\dots \\
&\quad \dots\int P_\theta p_\theta(\Omega)A^*_{\iota,\theta}(\Omega)A_{\iota',\theta}(\Omega) \\
&\quad +P_\phi p_\phi(\Omega)A^*_{\iota,\phi}(\Omega)A_{\iota',\phi}(\Omega)\mathrm{d}\Omega,
\end{aligned}
\tag{6.12}
$$

which concludes the proof. □

Appendix C. Derivation of Lemma 1

Proof. The spherical vector wave multimode expansion coefficients are given by (3.2)-(3.4), where we have assumed a mixed field with both random Gaussian, unpolarized, field components and one deterministic, polarized, field component. The

Gaussianity of the multipole modes follows directly from the Gaussianity assumption of the incident field and the fact that Gaussian variables remain Gaussian under summation and affine transformations in general.

The mean is directly obtained from the fact that the average of the expansion coefficients corresponding to the unpolarized waves is zero, $\langle f_\iota^{\mathrm{unpol}}\rangle = 0$. Hence, the average of the expansion coefficients is given by

$$\langle f_\iota \rangle = \frac{4\pi(-\mathrm{i})^{l-\tau+1}}{k\sqrt{2\eta}} \langle \boldsymbol{E}_0 \cdot \boldsymbol{A}_\iota^* \rangle = f_\iota^{\mathrm{pol}}. \tag{6.13}$$

The second moment of the mode distribution follows from Proposition 1 by considering the diagonal elements of correlation matrix for the expansion coefficients, i.e. the mode correlation. Hence, the second moment or the mode power can be expressed as the sum of the mode power corresponding to the linearly polarized ($\psi = 0$) and the unpolarized components

$$\langle f_\iota^* f_\iota \rangle = P_\iota = P_\iota^{\mathrm{pol}} + P_\iota^{\mathrm{unpol}}, \tag{6.14}$$

where $P_\iota = \mathcal{R}_{\iota\iota}$, $P_\iota^{\mathrm{pol}} = \mathcal{R}_{\iota\iota}^{\mathrm{pol}}$ and $P_\iota^{\mathrm{unpol}} = \mathcal{R}_{\iota\iota}^{\mathrm{unpol}}$. □

Appendix D. Proof of Proposition 2

Proof. From (4.6) we can write the total power of the outgoing signals from the N-port antenna

$$\begin{aligned} \|\boldsymbol{w}\|_F^2 &= \|\mathbf{R}\boldsymbol{a}\|_F^2 \\ &= \sum_n \left| \sum_\iota R_{n,\iota} a_\iota \right|^2, \end{aligned} \tag{6.15}$$

where we have introduced the multi–index $\iota \to \{\tau m l\}$, ordered and identified with the number $\iota = 2(l^2+l-1+m)+\tau$. By the Cauchy-Schwartz-Buniakovskii inequality

$$\|\boldsymbol{w}\|_F^2 \leq \sum_n \sum_\iota |R_{n,\iota}|^2 \, \|\boldsymbol{a}\|_F^2 \,. \tag{6.16}$$

Equality is achieved for $R_{n,\iota} = c_n a_\iota^*$, where c_n is a constant. From (4.1) and using normalization, $|v_n|^2 = 1$ and

$$\frac{1}{2\eta k^2} \int \boldsymbol{F}_n(\hat{\boldsymbol{r}}) \cdot \boldsymbol{F}_n^*(\hat{\boldsymbol{r}}) \mathrm{d}\Omega = 4\pi\eta_n, \tag{6.17}$$

we get for the transmission coefficients

$$\sum_\iota |T_{\iota,n}|^2 = 4\pi\eta_n. \tag{6.18}$$

Using the Lorentz condition for reciprocal antennas (4.5) we find out the constants c_n

$$c_n = \mathrm{e}^{\mathrm{i}\varphi_n} \frac{4\pi\eta_n}{\|\boldsymbol{a}\|_F}, \tag{6.19}$$

where φ_n is an arbitrary phase. Then, we finally arrive at the inequality that concludes the proof

$$\|\boldsymbol{w}\|_F^2 \leq 4\pi \sum_{n=1}^{N} \eta_n \|\boldsymbol{a}\|_F^2 . \tag{6.20}$$

□

Appendix E. Proof of Proposition 5

Proof. Given the correlation matrix of outgoing waves

$$\boldsymbol{\mathcal{R}}_w = \mathbf{R}\boldsymbol{\mathcal{R}}_a\mathbf{R}^H, \tag{6.21}$$

perform the diagonalization, $\boldsymbol{\mathcal{R}}_a = \mathbf{U}\boldsymbol{\Lambda}_a\mathbf{U}^H$, which leads to

$$\boldsymbol{\mathcal{R}}_w = \mathbf{R}\mathbf{U}\boldsymbol{\Lambda}_a\mathbf{U}^H\mathbf{R}^H, \tag{6.22}$$

where $\mathbf{U}^{\infty\times\infty}$, $\boldsymbol{\Lambda}_a^{\infty\times\infty}$, now choose $\mathbf{R} = c\mathbf{U}_{a,N}^H$, where $\mathbf{U}_{a,N}$ is a matrix containing N first eigenvectors of $\mathbf{U}$, corresponding the ordered eigenvalues in $\boldsymbol{\Lambda}_a$

$$\begin{aligned} \boldsymbol{\mathcal{R}}_w &= |c|^2\, \mathbf{U}_{a,N}^H \mathbf{U}\boldsymbol{\Lambda}_a\mathbf{U}^H\mathbf{U}_{a,N} \\ &= |c|^2\, \boldsymbol{\Lambda}_{a,N}. \end{aligned} \tag{6.23}$$

Now, using the normalization $|v_n|^2 = 1$ and

$$\frac{1}{2\eta k^2}\int \boldsymbol{F}_n(\hat{\boldsymbol{r}})\cdot\boldsymbol{F}_n^*(\hat{\boldsymbol{r}})\mathrm{d}\Omega = 4\pi\eta_n, \tag{6.24}$$

we get for the transmission coefficients

$$\sum_{\iota} |T_{\iota,n}|^2 = 4\pi\eta_n, \tag{6.25}$$

where we have made use of the multi–index notation, $\iota \to \{\tau m l\}$, ordered and identified with the number $\iota = 2(l^2 + l - 1 + m) + \tau$. Hence, since

$$\mathbf{R}\mathbf{R}^H = |c|^2\, \mathbf{U}_{a,N}^H\mathbf{U}_{a,N} = |c|^2\, \mathbf{I}_N, \tag{6.26}$$

and

$$\mathrm{tr}\mathbf{R}\mathbf{R}^H = |c|^2 N = 4\pi\sum_{n=1}^{N}\eta_n, \tag{6.27}$$

we get for the final result

$$\mathbf{R} = \mathrm{e}^{\mathrm{i}\varphi}\left(\frac{4\pi}{N}\sum_{n=1}^{N}\eta_n\right)^{\frac{1}{2}} \mathbf{U}_{a,N}^H. \tag{6.28}$$

□

References

[1] http://www.efieldsolutions.com/.

[2] A. Alayon Glazunov, A. F. Molisch, and F. Tufvesson. On the mean effective gain of antennas. Technical Report LUTEDX/(TEAT-7161)/1–23/(2007), Lund University, Department of Electrical and Information Technology, P.O. Box 118, S-221 00 Lund, Sweden, 2008. `http://www.es.lth.se/teorel`, Submitted to IET Microwave Antennas and Propagation.

[3] H. Asplund, A. Alayon Glazunov, A. F. Molisch, K. I. Pedersen, and M. Steinbauer. The cost 259 directional channel model-part ii: Macrocells. *Wireless Communications, IEEE Transactions on*, **5**(12), 3434–3450, December 2006.

[4] P. A. Bello. Characterization of randomly time-variant linear channels. *IEEE Transactions*, pages 360–393, December 1963.

[5] L. Chu. Physical limitations of omni-directional antennas. *Appl. Phys.*, **19**, 1163–1175, December 1948.

[6] R. T. Compton JR. The tripole antenna: An adaptive array with full polarization flexibility. *Antennas and Propagation, IEEE Transactions on*, **AP-29**(6), 944–952, November 1981.

[7] L. Correia, editor. *COST 273 final report: Towards mobile broadband multimedia networks.* Elsevier, 2006.

[8] R. Fano. Theoretical limitations on the broadband matching of arbitrary impedances. *Journal of the Franklin Institute*, **249(1,2)**, 57–83 and 139–154, Jan/Feb 1950.

[9] B. H. Fleury. First- and second-order characterization of direction dispersion and space selectivity in the radio channel. *IEEE Transactions on Information Theory*, **46**, 2027–2044, September 2000.

[10] G. J. Foschini and M. J. Gans. On limits of wireless communications in fading environments when using multiple antennas. *Wireless Personal Communications*, **6**, 311–335, 1998.

[11] M. Gustafsson and S. Nordebo. Characterization of mimo antennas using spherical vector waves. *Antennas and Propagation, IEEE Transactions on*, **54**(9), 2679–2682, Sept. 2006.

[12] M. Gustafsson and S. Nordebo. On the spectral efficiency of a sphere. *Progress In Electromagnetics Research*, **PIER 67**, 275–296, 2007.

[13] L. Hanlen and M. Fu. Wireless communication systems with-spatial diversity: a volumetric model. *Wireless Communications, IEEE Transactions on*, **5**(1), 133–142, Jan. 2006.

[14] L. W. Hanlen and R. C. Timo. Intrinsic capacity of random scattered spatial communication. In *Information Theory Workshop, 2006. ITW '06 Chengdu. IEEE*, pages 281–285, Oct. 2006.

[15] J. E. Hansen, editor. *Spherical Near-Field Antenna Measurements.* London, U.K., Peter Peregrinus, 1988.

[16] T. Hansen and A. Yaghijan. *Plane-Wave Theory of Time-Domain Fields:Near-Field Scanning Applications".* Wiley-IEEE press, May 1999.

[17] W. W. Hansen. A new type of expansion in radiating problems. *Phys. Review*, **47**, 139–143, Jan. 1935.

[18] W. C. Jakes. *Microwave Mobile Communications.* IEEE Press, 1974.

[19] J. Jensen, M.A.; Wallace. A review of antennas and propagation for mimo wireless communications. *Antennas and Propagation, IEEE Transactions on*, **52**(11), 2810–2824, Nov. 2004.

[20] S. Loyka. Information theory and electromagnetism: Are they related? In *International Symposium on Antenna Technology and Applied Electromagnetics (ANTEM'04), Ottawa, Canada,*, Jul. 20-23 2004.

[21] A. F. Molisch. *Wireless Communications.* IEEE Press, Wiley, 2005.

[22] A. Papoulis. *Probability, Random Variables and Stochastic Processes.* Number ISBN 0-07-048477-5 in International Edition. Mc Graw-Hill International Edition, 1991.

[23] T. Pollock, T. Abhayapala, and R. Kennedy. Spatial limits to MIMO capacity in general scattering environments. In *7th International Symposium on DSP for Communication Systems*, pages 49–54, Dec. 2003.

[24] T. S. Pollock, T. D. Abhayapala, and R. A. Kennedy. Introducing space into MIMO capacity calculations. *Journal on Telecommunications Systems*, **24**(2), 415–436, 2003.

[25] T. Svantesson. An antenna solution for mimo channels: the multimode antenna. In *Signals, Systems and Computers, 2000. Conference Record of the Thirty-Fourth Asilomar Conference on*, volume 2, pages 1617–1621vol.2, 29 Oct.-1 Nov. 2000.

[26] T. Svantesson. On the potential of multimode antenna diversity. In *Vehicular Technology Conference, 2000. IEEE VTS-Fall VTC 2000. 52nd*, volume 5, pages 2368–2372vol.5, 24-28 Sept. 2000.

[27] T. Taga. Analysis for mean effective gain of mobile antennas in land mobile radio environments. *Vehicular Technology, IEEE Transactions on*, **39**(2), 117–131, May 1990.

[28] I. E. Telatar. Capacity of multi-antenna Gaussian channels. *European Transactions on Telecommunications*, **10**, November–December 1999.

Andrés Alayón Glazunov, Mats Gustafsson, Andreas F. Molisch, and Fredrik Tufvesson, "Physical Modeling of MIMO Antennas and Channels by Means of the Spherical Vector Wave Expansion,"
LUTEDX/(TEAT-7177)/1-31/(2009).

Andreas D. Ioannidis, Daniel Sjöberg, and Gerhard Kristensson, "On the propagation problem in a metallic homogeneous biisotropic waveguide,"
LUTEDX/(TEAT-7178)/1-27/(2009).

Anders Karlsson, Henrik Bladh, and Per-Erik Bengtsson, "An accurate method for predicting light scattering from soot aggregates with sub-particles of arbitrary shape and structure,"
LUTEDX/(TEAT-7179)/1-22/(2009).

Sven Nordebo, Andreas Fhager, Mats Gustafsson, Börje Nilsson, "Fisher information integral operator and spectral decomposition for inverse scattering problems,"
LUTEDX/(TEAT-7180)/1-21/(2009).

Mats Gustafsson, "Sum rule for the transmission cross section of apertures in thin opaque screens,"
LUTEDX/(TEAT-7181)/1-8/(2009).

Christer Larsson, Mats Gustafsson, and Gerhard Kristensson, "Wideband microwave measurements of the extinction cross section—Experimental techniques,"
LUTEDX/(TEAT-7182)/1-22/(2009).

Daniel Sjöberg and Mats Gustafsson, "Realization of a matching region between a radome and a ground plane,"
LUTEDX/(TEAT-7183)/1-6/(2010).

Kristin Persson, Mats Gustafsson, and Gerhard Kristensson, "Reconstruction and visualization of equivalent currents on a radome using an integral representation formulation,"
LUTEDX/(TEAT-7184)/1-45/(2010).

Mats Gustafsson, "Time-domain approach to the forward scattering sum rule,"
LUTEDX/(TEAT-7185)/1-14/(2010).

Mats Gustafsson and Daniel Sjöberg, "Sum rules and physical bounds on passive metamaterials,"
LUTEDX/(TEAT-7186)/1-19/(2010).

Mats Gustafsson, "Accurate and efficient evaluation of modal Green's functions,"
LUTEDX/(TEAT-7187)/1-10/(2010).

Alireza Kazemzadeh and Anders Karlsson, "Multilayered Wideband Absorbers for Oblique Angle of Incidence,"
LUTEDX/(TEAT-7188)/1-18/(2010).

Alireza Kazemzadeh and Anders Karlsson, "Nonmagnetic Ultra Wideband Absorber with Optimal Thickness,"
LUTEDX/(TEAT-7189)/1-14/(2010).

Daniel Sjöberg and Christer Larsson, "Cramér-Rao bounds for determination of permittivity and permeability in slabs,"
LUTEDX/(TEAT-7190)/1-13/(2010).

Anders Karlsson and Alireza Kazemzadeh, "On the Physical Limit of Radar Absorbers,"
LUTEDX/(TEAT-7191)/1-10/(2010).

Alireza Kazemzadeh, "Thin Wideband Absorber with Optimal Thickness,"
LUTEDX/(TEAT-7192)/1-9/(2010).

Anders Bernland, Annemarie Luger and Mats Gustafsson, "Sum Rules and Constraints on Passive Systems,"
LUTEDX/(TEAT-7193)/1-28/(2010).

Anders Bernland, Mats Gustafsson, and Sven Nordebo, "Physical Limitations on the Scattering of Electromagnetic Vector Spherical Waves,"
LUTEDX/(TEAT-7194)/1-23/(2010).

Mats Gustafsson, "Polarizability and physical bounds on antennas in cylindrical and rectangular geometries,"
LUTEDX/(TEAT-7195)/1-11/(2010).

Christer Larsson, Daniel Sjöberg, and Lisa Elmkvist, "Waveguide measurements of the permittivity and permeability at temperatures up to 1000 °C,"
LUTEDX/(TEAT-7196)/1-22/(2010).

Andreas Ioannidis, "On the cavity problem for the general linear medium in Electromagnetic Theory,"
LUTEDX/(TEAT-7197)/1-13/(2010).

Mats Gustafsson and Daniel Sjöberg, "Physical bounds and sum rules for high-impedance surfaces,"
LUTEDX/(TEAT-7198)/1-17/(2010).

Daniel Sjöberg, Mats Gustafsson, and Christer Larsson, "Physical bounds on the all-spectrum transmission through periodic arrays: oblique incidence,"
LUTEDX/(TEAT-7199)/1-13/(2010).

Mats Gustafsson, Marius Cismasu, and Sven Nordebo, "Absorption Efficiency and Physical Bounds on Antennas,"
LUTEDX/(TEAT-7200)/1-20/(2010).

Ruiyuan Tian, Buon Kiong Lau, and Zhinong Ying, "Characterization of MIMO Antennas with Multiplexing Efficiency,"
LUTEDX/(TEAT-7201)/1-6/(2010).

Andreas D. Ioannidis, Gerhard Kristensson, and Ioannis G. Stratis, "On the well-posedness of the Maxwell system for linear bianisotropic media,"
LUTEDX/(TEAT-7202)/1-25/(2010).

Gerhard Kristensson, "The polarizability and the capacity change of a bounded object in a parallel plate capacitor,"
LUTEDX/(TEAT-7203)/1-39/(2010).